(12)

CHEMICAL
RESEARCH,
DEVELOPMENT &
ENGINEERING
CENTER

CRDEC-TR-407

INTERPRETATION OF ADSORPTION ISOTHERM HYSTERESIS FOR AN ACTIVATED CHARCOAL USING STOCHASTIC PORE NETWORKS

R. Mann
H. Yousef

DEPARTMENT OF CHEMICAL ENGINEERING
UMIST, England

D.K. Friday

GEO-CENTERS, INC.
Fort Washington, MD 20744

J.J. Mahle

RESEARCH DIRECTORATE

September 1992

U.S. ARMY
ARMAMENT
MUNITIONS
CHEMICAL COMMAND

Aberdeen Proving Ground, Maryland 21010-5423

Disclaimer

The findings in this report are not to be construed as an official Department of the Army position unless so designated by other authorizing documents.

REPORT DOCUMENTATION PAGE

Form Approved
OMB No. 0704-0188

1. AGENCY USE ONLY (Leave blank)	2. REPORT DATE	3. REPORT TYPE AND DATES COVERED
	1992 September	Final, 91 Jun - 91 Nov

4. TITLE AND SUBTITLE
Interpretation of Adsorption Isotherm Hysteresis for an Activated Charcoal Using Stochastic Pore Networks

5. FUNDING NUMBERS
PR-10161102A71A

6. AUTHOR(S)
Mann, R.; Yousef, H. (Department of Chemical Engineering); Friday, D.K. (GEO-CENTERS, Inc.); and Mahle, J.J. (CRDEC)

7. PERFORMING ORGANIZATION NAME(S) AND ADDRESS(ES)
Department of Chemical Engineering, UMIST, Manchester M60 1QD, England
GEO-CENTERS, Inc., Fort Washington, MD 20744
CDR, CRDEC, ATTN: SMCCR-RSC-A, APG, MD 21010-5423

8. PERFORMING ORGANIZATION REPORT NUMBER
CRDEC-TR-407

9. SPONSORING/MONITORING AGENCY NAME(S) AND ADDRESS(ES)

10. SPONSORING/MONITORING AGENCY REPORT NUMBER

11. SUPPLEMENTARY NOTES

12a. DISTRIBUTION/AVAILABILITY STATEMENT
Approved for public release; distribution is unlimited.

12b. DISTRIBUTION CODE

13. ABSTRACT (Maximum 200 words)

Water vapor adsorption equilibria on activated carbons typically exhibit hysteresis. The size and shape of the hysteresis loop which separates the adsorption and desorption branches is a strong function of the pore size and interconnectivity of the pore. Neither conventional pore filling models nor statistical thermodynamics approaches provide a means for predicting the extent of hysteresis from only adsorption measurements. This work uses the Kelvin Equation in conjunction with the structural concept of a stochastic network to describe measured water isotherms on BPL carbon.

14. SUBJECT TERMS
Network models
Adsorption hysteresis
Water vapor adsorption

15. NUMBER OF PAGES
35

16. PRICE CODE

17. SECURITY CLASSIFICATION OF REPORT	18. SECURITY CLASSIFICATION OF THIS PAGE	19. SECURITY CLASSIFICATION OF ABSTRACT	20. LIMITATION OF ABSTRACT
UNCLASSIFIED	UNCLASSIFIED	UNCLASSIFIED	UL

Blank

PREFACE

The work described in this report was authorized under Project No. 10161102A71A, Research in CW/CB Defense. This work was started in June 1991 and completed in November 1991.

The use of trade names or manufacturers' names in this report does not constitute an official endorsement of any commercial products. This report may not be cited for purposes of advertisement.

This report has been approved for release to the public.

Blank

CONTENTS

LIST OF FIGURES AND TABLES

Figure No.

Table

INTERPRETATION OF ADSORPTION ISOTHERM HYSTERESIS FOR AN ACTIVATED CHARCOAL USING STOCHASTIC PORE NETWORKS

1. INTRODUCTION

Activated carbon is used in countless industrial hygiene and air purification applications. It is important to understand the nature of water adsorption, since in air with non-zero relative humidity, the presence of water inevitably interferes with the concurrent take-up of any toxic or contaminant compounds in the air.

For adsorbents like activated carbon, it is widely recognized that the extent of sorbate take-up is some combination of surface adsorption and capillary condensation. For water adsorption from humid air, experiments show a pronounced hysteresis between the adsorption and desorption branches of the isotherm[1]. This hysteresis is suspected to be structurally linked. So far, however, there is no convincing explanation of how the pore space geometry, interior spatial topology and surface texture of an activated carbon can be quantitatively related to adsorption isotherm hysteresis. Grossly simplistic concepts such as the ink bottle explanation[2], are self-evidently inadequate in representing the seemingly intractable complexities of a porous carbon adsorbent simultaneously exhibiting micro-, meso- and macroporosity.

The concept of random or stochastic networks of simple pores has been available for some time, following the pioneering work by Fatt[3]. Applications to adsorption using 3-D networks was significantly advanced by Nicholson and Petropoulos[4]. More recently, the crucial impact of the pore size distribution on adsorption isotherm hysteresis has been demonstrated by Thomson and Mann[5]. Also more recently, Petropoulos, et al[6] have shown how under partially filled conditions a stochastic network exhibits complex interactions of uptake and permeability. More generally, simple stochastic pore networks have been shown to be capable of explaining a wide variety of phenomena in porous materials, including hysteresis in mercury porosimetry[7,8], low recovery in water flood oil displacement[9], catalyst tortuosity under reaction and non-reaction conditions[10], catalyst deactivation by coke laydown[11,12] and effective diffusivity in Wicke-Kallenbach experiments[13].

Stochastic pore networks have been devised as a computationally tractable quantitative treatment of the random interconnected pore spaces encountered in typical porous materials. In this work, we demonstrate their application to a specific sample water isotherm in a BPL carbon showing pronounced isotherm hysteresis. The interconnections amongst and between pores of variable sizes seemingly jumbled randomly together, present a simple explanation of the degree of hysteresis observed. Pictorialisations of the deduced networks, albeit only in 2-D and of restricted size amounting to assemblies of pores of the order of thousands,

show how the 'texture' of the pore spaces can be visually presented. It is intended ultimately that stochastic pore networks configured by fractal geometry should provide an SEM image reconstruction basis for pore structure evaluation[14], thereby dispensing with the perpetual necessity to undertake difficult laboratory procedures which in themselves only provide an indirect measure of the detailed morphology of typically highly complex pore spaces.

Activated carbon is used in countless industrial hygiene and air purification applications for removal of organic vapors. In many cases, however, water vapor is present in high concentrations with high adsorption loadings.

2. FILLING AND EMPTYING OF A SINGLE PORE

The process of capillary condensation for an 'idealised' cylindrical pore is shown in Fig. 1. The amount of gas adsorbed in such an idealised geometry can be readily calculated from an understanding of the thickness of the adsorbed layer and the Kelvin Equation. The pressure p at which such a pore will fill with condensed gas is given by:

$$r - t = \frac{-2\sigma V_L \cos\theta}{RT \ln\left(\frac{p}{p_{sat}}\right)} \qquad (1)$$

In these circumstances as the pressure of the adsorbing gas is raised from zero to p_{sat} and returned back to zero, there will be a small hysteresis between the adsorption and desorption branches of the isotherm caused by the fact that the pore will empty at a lower pressure since the thickness of the adsorbed layer does not affect the meniscus curvature at the pore emptying pressure[5]. In the event that the thickness t of the adsorbed layer is small relative to the pore radius, any hysteresis effect between adsorption and desorption will be vanishingly small. For porous materials which show a large hysteresis effect, other mechanisms must be sought to explain the widely different paths exhibited by the adsorption and desorption branches of the isotherm.

3. FILLING AND EMPTYING OF A SIMPLE NETWORK OF PORES

Fig. 2 shows a pictorialisation of a simple network of idealised cylindrical pores of size 4 x 4. This network contains pores distributed between 0 and 1000 Å and is related to one previously used by Mann and Thomson[5] to demonstrate how accessibility limitations in a pore network may give pronounced isotherm hysteresis. Using data for water[1] gives the predicted isotherm behaviour depicted in Fig. 3.

The filling of the larger pores is deferred until the dimensionless pressure p/p_{sat} has exceeded 0.8. Thus 95% of the pore volume is filled with condensate as relative pressure increases from 0.86 to 0.89. This corresponds to pores of size 750 to 971 Å.

On reducing the relative pressure from the condition where all the pores are filled, those large pores located on the outside of the network empty at pressures corresponding to their radius. However, there are some 13 pores which are shielded behind smaller pores. They cannot be emptied of condensate until the pressure has fallen sufficiently to empty the shielding pores. This occurs at a relative pressure of 0.55 and produces a sudden reduction in the volume of water adsorbed. Fig. 3 shows a most pronounced hysteresis between the filling and emptying process for this simple network. The full sequence of filling and emptying on a pore by pore basis is shown in Table.

4. FITTING A NETWORK TO AN ADSORPTION ISOTHERM

It is a simple enough matter to construct networks of any size and to compose them with any possible distribution of pore segments. Fig. 4 shows a pictorialised example of a 20 x 20 network which comprises uniformly distributed pores between 10 and 4400 Å with a node spacing of 20,000 Å. In Fig. 4, the pores which obey a uniform distribution have been placed randomly within the network. This means that the size of a given pore is statistically independent of the size of its neighbouring pores. This is termed a stochastic pore network.

The second problem in developing applications of stochastic pore networks is to deduce the statistical distribution of pore segment sizes from a given characterisation method. In this respect, Fig. 5 shows the experimental adsorption/desorption isotherms for a sample of BPL carbon. Fortunately, it is always possible to directly deduce the pore segment distribution for the process of adsorption, since there are no accessibility limitations during capillary filling by condensation. All pores, irrespective of their radius or position in a network, will fill at a relative pressure dictated by the Kelvin Equation (Eq (1)).

A stochastic network is then constructed from the adsorption branch in Fig. 5 by dividing the cumulative volume ordinate into (say) 10 equal volume increments. The first volume increment from 0 to 0.1 must comprise pores between zero and 156 Å in diameter, since the relative pressure abscissa of 0.48 corresponds to the upper limit of pore size in this incremental volume range. Pore segments are then assumed to be uniformly distributed in this range. The second volume increment (between 0.1 and 0.2) then extends to a relative pressure of 0.54 which must correspond to pores with radii between 156 Å and 185 Å. This argument is applied

to each volume increment in turn up to a cumulative volume of 1.0 which obviously corresponds to a complete filling of the network.

The result of this procedure is to provide relative numbers of pores obeying a uniform distribution in each of the ten pore radii ranges. The actual number of pores to be allocated in each of these size ranges is then determined by the size of network to be constructed. The overall numbers of pores have to be coincident with the $2N(N+1)$ pores that form an N x N stochastic network of pores.

Networks of size 20 x 20 form convenient visualisations in 2-D on a PC screen, thereby enabling an image based assessment of the character of the stochastic network. The 20 x 20 network has 840 pores in total. The fitting to the experimental water isotherm in Fig. 5 by the above procedures gives the result depicted in Fig. 6 which shows the 840 pores sizes individually as placed randomly in the network. Fig. 7 then shows a pictorialisation of the network of Fig. 6. The corresponding number distribution and volume distribution histograms are presented in Figs. 8(a) and 8(b) respectively. The juxtaposition of the two figures is striking, since it is immediately evident that the majority of the pore volume is contained in just a few large pores. In fact of the total 840 pores, the five largest pores have radii of 1795, 564, 560, 556, and 542, which account for some 14% of the total network volume. In contrast, 90% by number of the pores have sizes less than 300 Å. It is not immediately obvious, but the accessibility of the few large pores is controlled by the preponderance of much smaller pores. It is inevitable that a large proportion of the larger pores will be hidden amongst smaller ones and this could be expected to lead to a pronounced hysteresis effect.

5. PREDICTING THE DESORPTION BRANCH OF THE ISOTHERM

Once the network in Fig. 6 has been completely filled by condensate, the emptying process, on reduction of the water pressure, will initiate from the largest pore on the exterior. This is of size 541 Å located at row 32 and column 21. No further emptying occurs because the neighbour pores are of sizes 221, 211 and 26 Å. This single emptying step takes place at a relative pressure of 0.81. The desorption process is followed step by step. A significant hysteresis loop is generated because the largest proportion of the larger pores are shielded amongst smaller pores. The full desorption (or emptying) branch is presented in Fig. 9 for the detailed calculation of the entire 840 pores.

As can be seen from Fig. 9, the non-emptying of large hidden pores initially causes the predicted desorption to lie above the experimental result for random placement of pores. However, at around a relative pressure of 0.55, corresponding to the emptying of pores of radius 189 Å, there occurs a very large emptying of a set of connected pores which causes the desorption branch to fall suddenly below

the experimental result. In qualitative terms, this behaviour is linked to the percolation threshold of those pores lying below the size of 189 Å. The result is that some 70% of the whole network dimensionless volume empties as the relative pressure falls from 0.55 to 0.44. Below this percolation type threshold, there is almost negligible shielding possibility of large pores behind small ones. As a result the desorption branch becomes closely coincident with the adsorption one, so that they are effectively indistinguishable.

If these simulations are now carried out for a network of double the size, i.e. a 40 x 40 network comprised of 3280 pores, there is of course little visually detectable change in the adsorption branch of the isotherm. However, because of the increased potential for shielding of large pores behind smaller ones, the desorption branch is always significantly displaced above that for the smaller 20 x 20 network. As a result, although the hysteresis loop is enlarged, the quality of fit to the experimental result is effectively made worse, especially in the relative pressure range from 0.55 down to 0.44. This comparison for 20 x 20 and 40 x 40 networks is shown in Fig. 10.

6. EFFECT OF STRUCTURE RE-ORDERING ON THE DESORPTION BRANCH

So far, the two networks examined have been entirely randomised, so that the size of a pore at any position is taken to be independent of the size of any neighbouring pores. If some order is to be introduced into the assembly of pores in forming a network, it is first of all quite clear that, irrespective of the nature of re-structuring, the adsorption (or filling) branch will be entirely unaffected. It is however evident that the effects of re-structuring from a random basis will show up in the desorption isotherm.

This can be easily demonstrated with respect to an illustrative extreme of re-ordering whereby the full set of random pores are assembled in rank order and then spirally 'wound' into position in the network. If the spiral rewinding places the largest pore at the centre and the smallest pore at the exterior, the pictorialised 20 x 20 network of Fig. 6 appears as shown in Fig. 11(a). This network, which has pore sizes graded in size from the outside to the centre will not empty of sorbate until the value of p/p_{sat} corresponds to the largest outside perimeter pore. For the set of pores from Fig. 6 this corresponds to a very small pore of radius 29 Å. At this extreme of ordered structure, the desorption branch appears as a step change as shown in Fig. 12. This represents the largest possible hysteresis. In contrast, the counterpart spirally wound network with the smallest pore at the centre and the largest on the exterior gives zero hysteresis, so that the desorption branch is exactly coincident everywhere with the adsorption. This network is pictorialised in Fig. 11(b) for the same 20 x 20 network as in Fig. 11(a) and Fig. 6 and the open

accessible nature of all the pores is immediately obvious.

It is therefore clear that a huge variation of possibilities for the desorption branch exists according to extents of restructuring which lie between complete randomness and the extreme of spiralling size ranked assembly.

Fig. 13 then shows an example of a close match of the experimental desorption branch which has been achieved by a small extent of structural reordering. This reordering has three conceptual components. These can be briefly summarised as (i) a preferred location of some of the largest pores on the exterior surface, (ii) a sub-surface layer comprised of a lower proportion of mid-size range pores and (iii) a small proportion of shielded voids in which some of the largest pores are isolated amongst some of the smallest ones. The structural reordering, which we term a patchy heterogeneity, leaves 95% of the pore network completely random, and requires the adjustment of only some 54 pores out of the total of 840 for a 20 x 20 network.

The full details of the structural re-ordering are presented in Fig. 14 in two parts. Fig. 14(a) shows the original locations of the 54 manipulated pores. The remainder of the pores in the network which are not affected are shown as asterisks. The size of these unaffected pores can be read from Fig. 6. Fig. 14(b) then indicates the nature of the changes made and shows the adjusted pores in their new positions. The three stages of adjustments are then as follows.

Firstly, in order to provide for an increased extent of desorption over the relative pressure range from 1.0 down to 0.7, the small number of pores sized from 541 Å down to 400 Å have been relocated on the network exterior. These 8 pores are indicated by enclosure in a single box in Fig. 14(b). The largest of these pores gives an initial desorption at a relative pressure o 0.82 with the remaining pores emptying down to a relative pressure of 0.75.This improves the initial fit of the isotherm (see Fig. 9 for comparison with the fully random network) which is indicative of an increased probability for larger pores to be located at the network exterior.

Secondly, the subsequent accelerated rate of emptying observed for the random network is avoided by replacing some of the exterior pores of size 390 Å down to 295 Åto more interior positions. These are shown underscored in Fig. 14(b) and amount to just 11 pores. These pores have been switched with 11 pores in the range 165 Ådown to 158 Åwhich have been replaced into the vacated 11 pore exterior portions. These pores which have been moved outward are shown as overscored in Fig. 14(b). This second phase of adjustment amounts to a tendency for the immediately inner layers of pores to be smaller on average than for the whole network. As a result of this adjustment, a steadily progressive desorption is

maintained from a relative pressure of 0.7 down to 0.5.

The third and final phase of heterogeneity involves the requirement to avoid a sudden onset of emptying related to a percolation threshold in the relative pressure range from around 0.5, so that there is still a significant water retention at a relative pressure as low as 0.4. This can be achieved by restricting the emptying of the five largest pores by surrounding them by smaller ones. Just three such "shielded voids" are necessary to achieve this and these are shown in large "boxed" conglomerates of pores in Fig. 14(b). The first to empty would be the largest 1795 Å pore surrounded by pores sized from 126 Å to 123 Å. The second conglomerate of 3 large pores forming a single void empties between 72 Å and 68 Å. The final shielded void with a pore size of 542 Å is shielded by very small pores of size 34 Å to 12 Å which empties at a relative pressure of 0.21. As a result of the creation of these three shielded voids, the final portion of the desorption emptying closely follows the experimental result.

Although the particular quantitative details of this restructuring should not be taken to possess precise significance, the concept of partial restructuring comprising a patchy heterogeneity, as distinct from exact randomness, may well be the appropriate qualitative concept to explain the desorption isotherm which has been experimentally measured. It is then possible that this concept of a patchy heterogeneity is related to the processing procedures which have resulted in the formation of the activated carbon particles. In any event, it is clear that partially ordered/partially random structures have the capability to explain and describe the water isotherm hysteresis encountered in this case.

Finally, for the deduced structure at a 20 x 20 size, it can be seen that the largest pore of size 1795 Å is still filled with water at 1/2 desorption, but empty when 3/4 of the desorption has taken place.

7. CONCLUSIONS

- The concept of a simple 2-D stochastic pore network of cylindrical pore segments can be readily applied to deduce the intrinsic pore segment distribution for a specific sample of a BPL activated charcoal. The deduction of the pore size distribution (psd) is simpler than for mercury porosimetry since in adsorption by capillary condensation, there are no accessibility limitations.

- The extent of hysteresis between adsorption and desorption has been shown to be attributed to the way pore segments are assembled together.

- The most extreme hysteresis between the adsorption and desorption

branches occurs when the pore sizes are spirally allocated into a network with the largest pores on the interior sequenced to the smallest pores on the exterior of the network.

- There is a negligible hysteresis for the reversed spiral assembly which has the largest pores on the outside of the network and the smallest ones at the centre.

- For the BPL studied, random assembly of pores produced only a poor approximation of the experimental hysteresis loop. An exact replication could be achieved by using a simple patchy heterogeneity which required manipulation of only 5% of the pores forming the network. This partial restructuring involved larger pores preferentially on the exterior, an inner layer with a smaller proportion of mid-size pores and a small number of shielded voids.

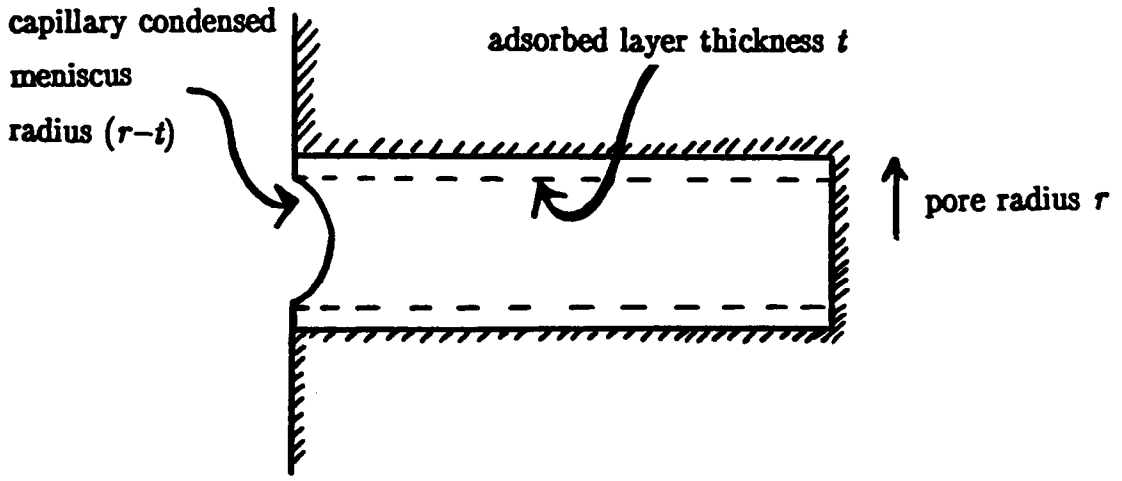

FIG.1 Simple single pore model

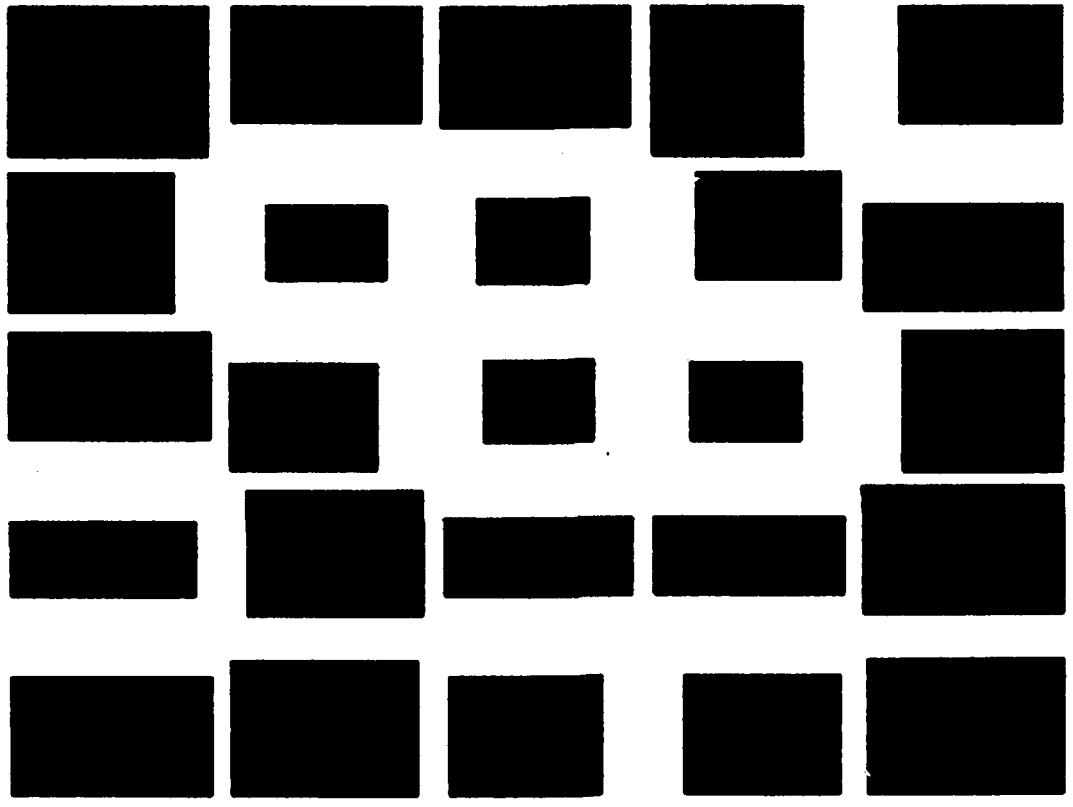

FIG.2 Pictorialisation of a simple 4 x 4 network

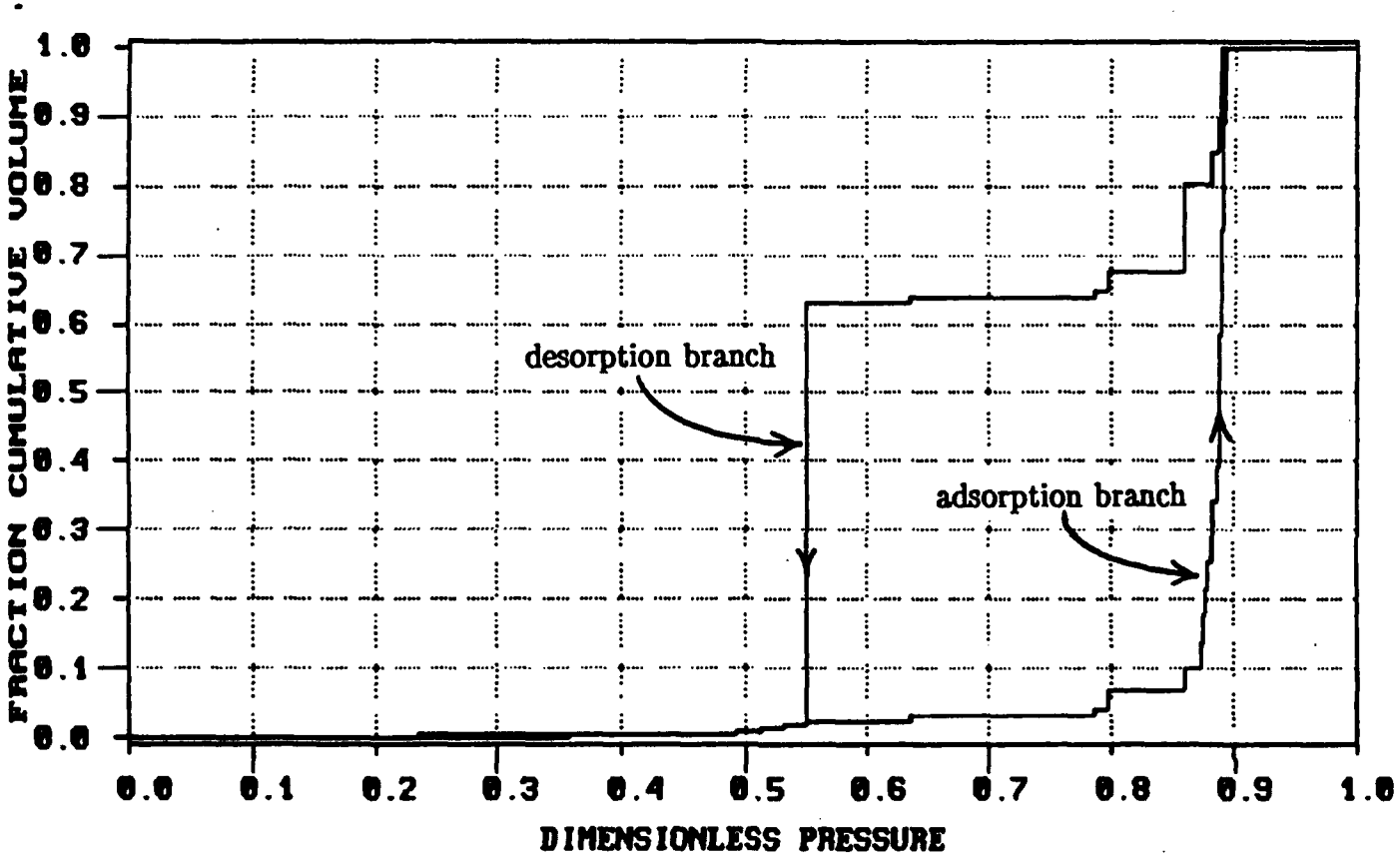

FIG.3 Water adsorption/desorption isotherms for network of Fig.2

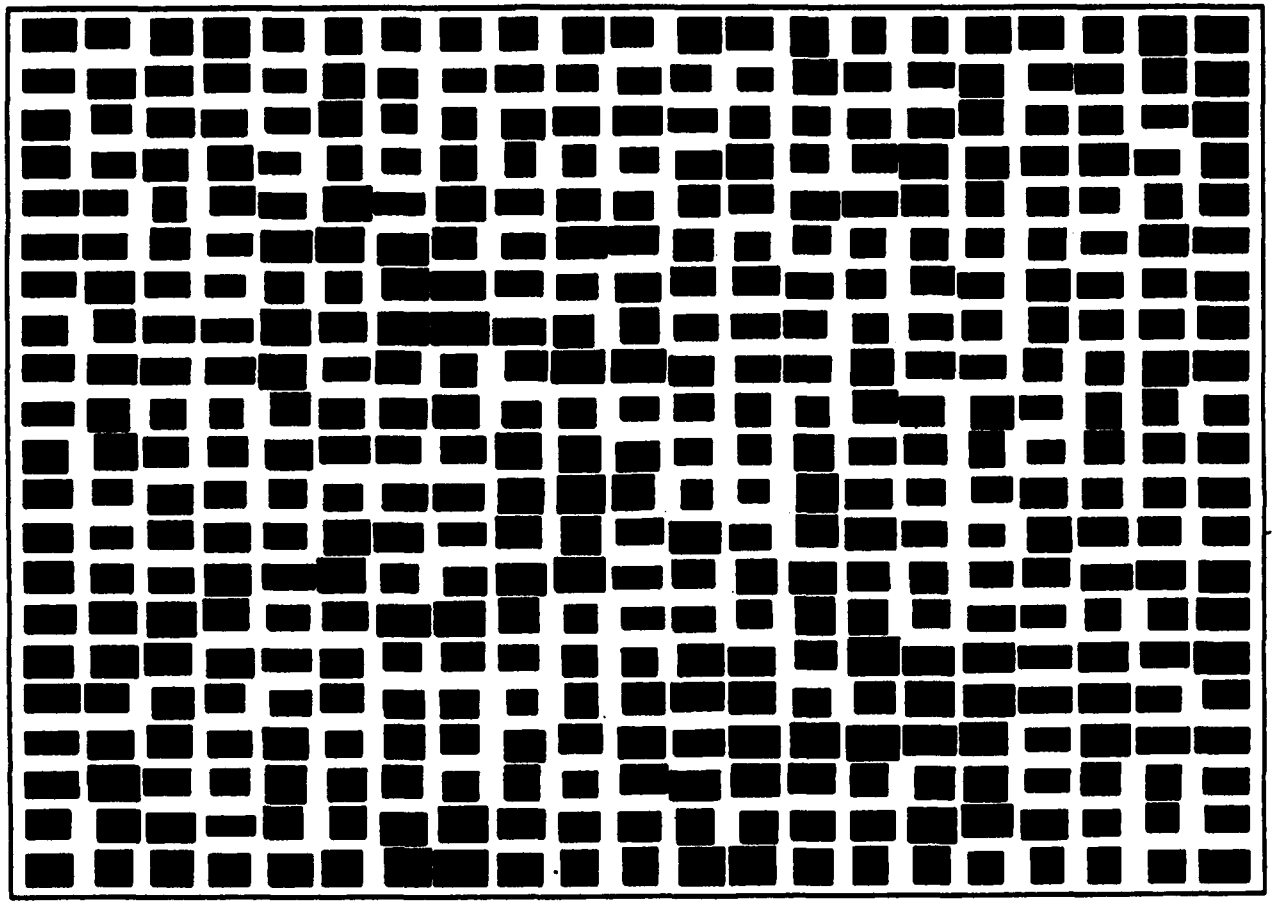

FIG.4 Pictorialised 20 x 20 network for uniform distribution of pore sizes

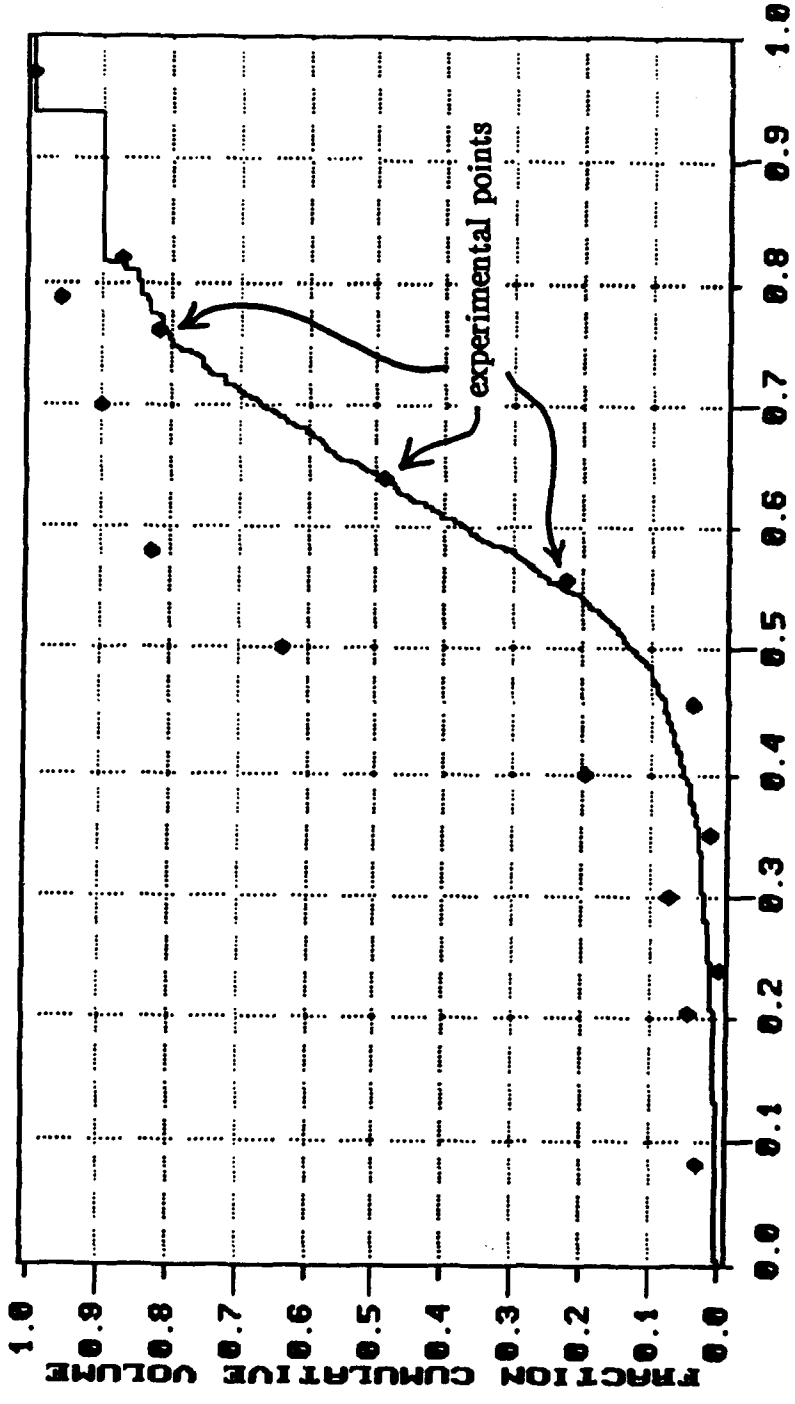

FIG.5 Experimental adsorption isotherm fitted by a random 20 x 20 network

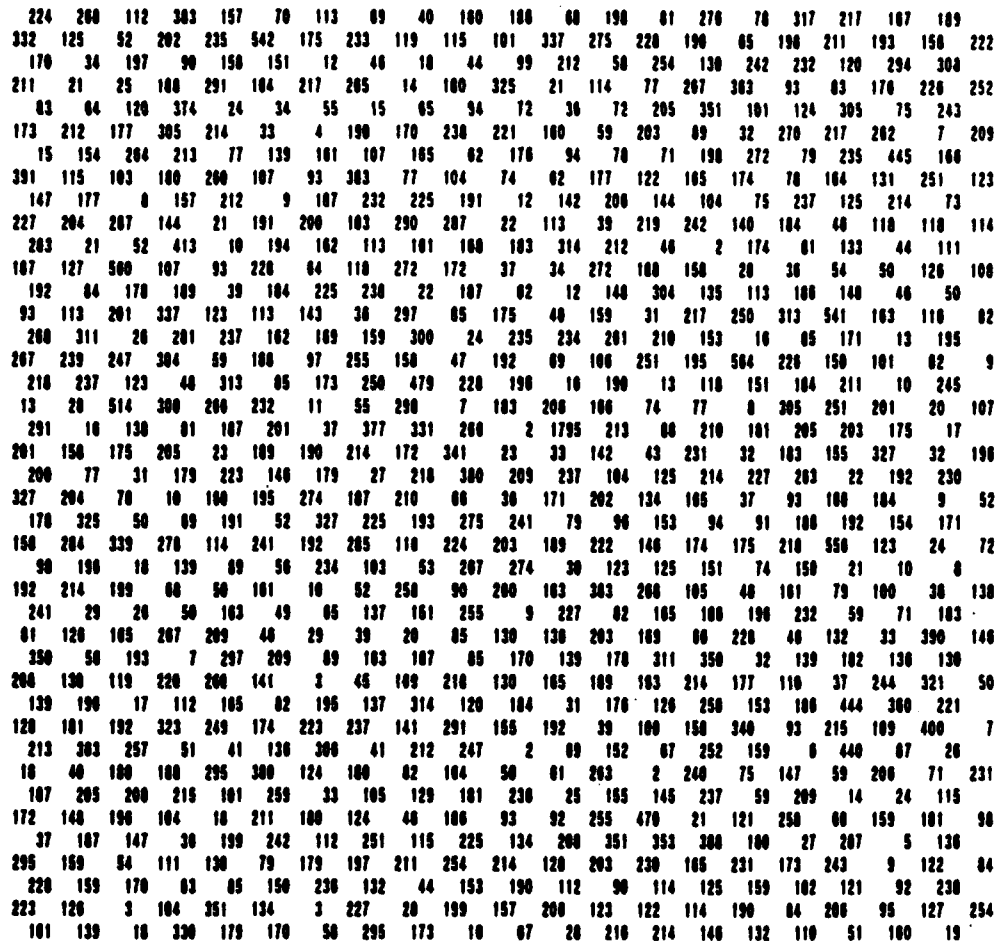

FIG.6 Numerical values of 840 pores in fitted random network (20 x 20)

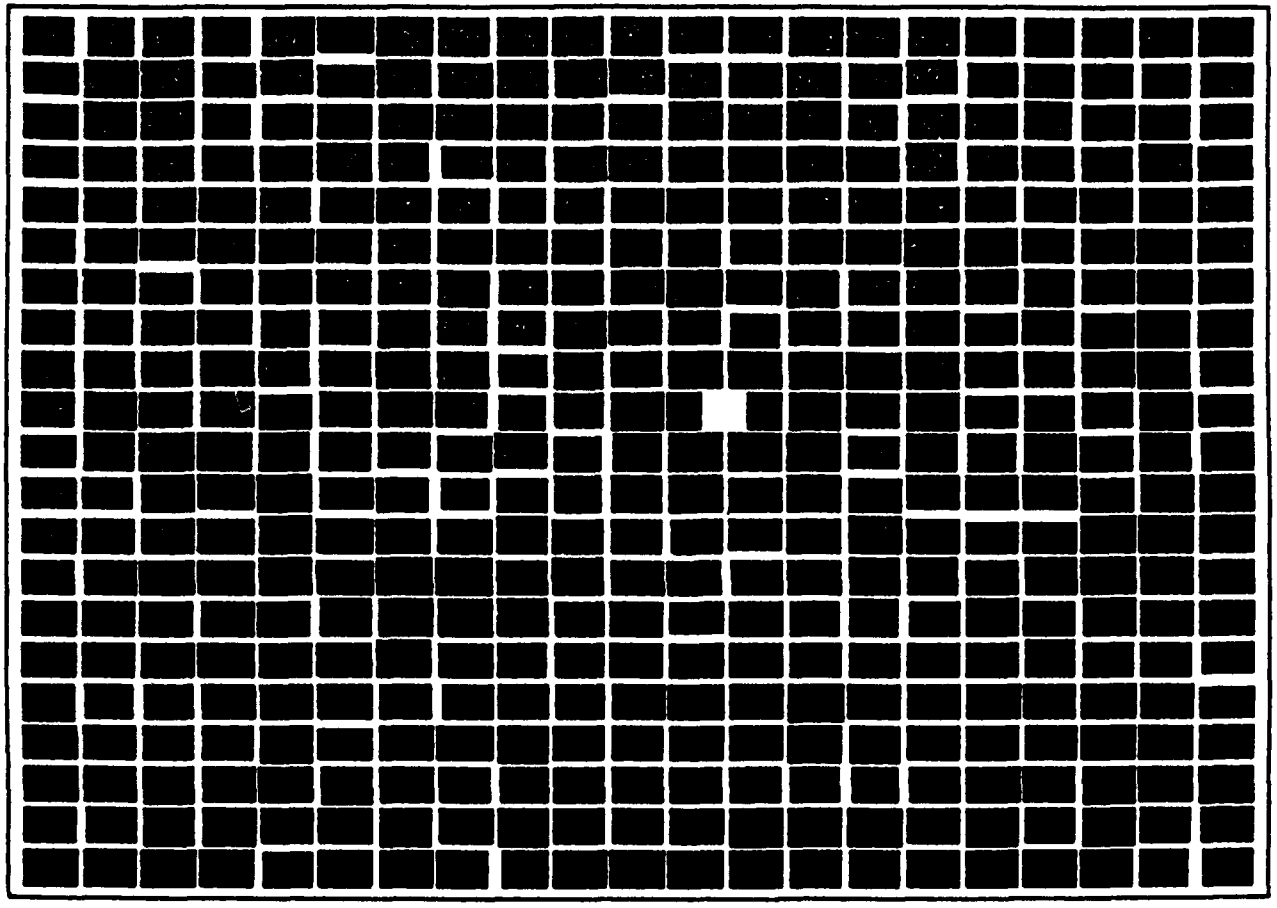

FIG.7 Pictorialisation of the fitted random network

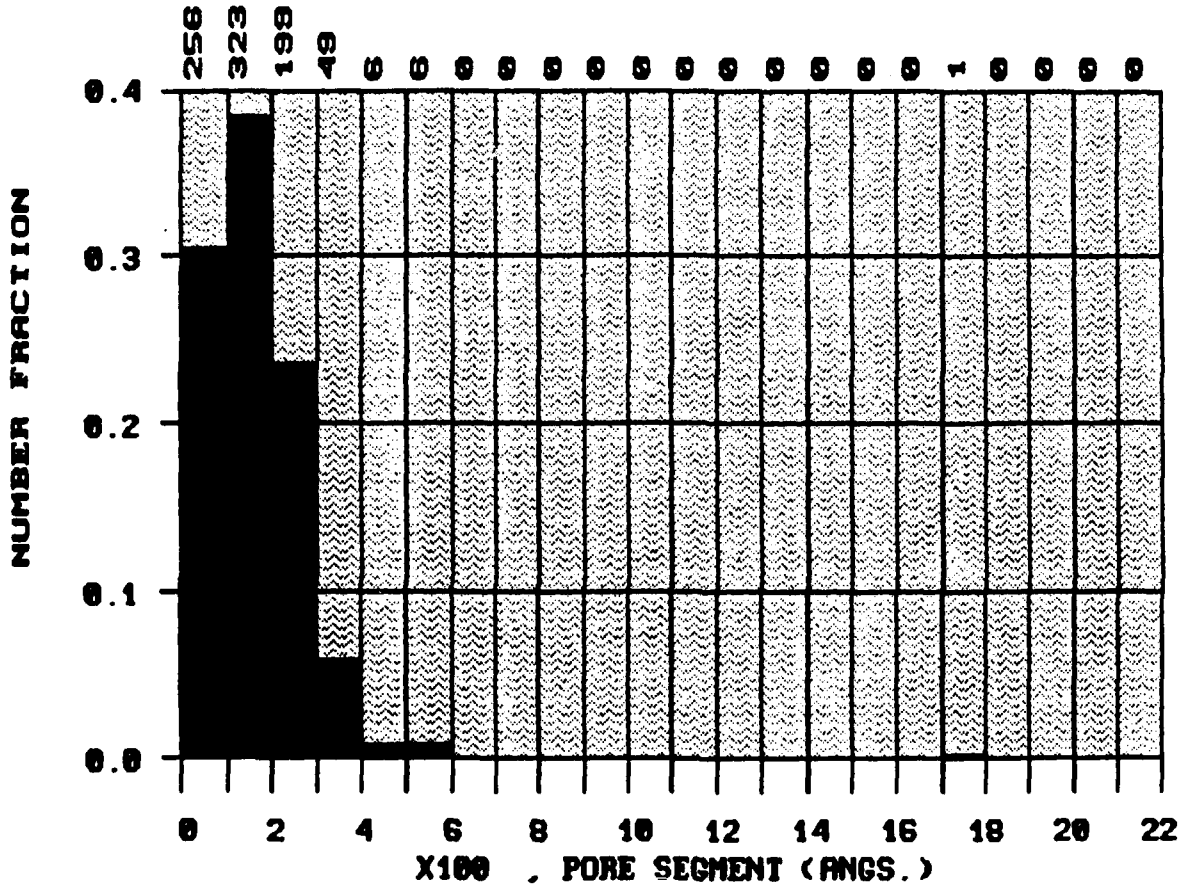

FIG.8(a) Number distribution of pore segments

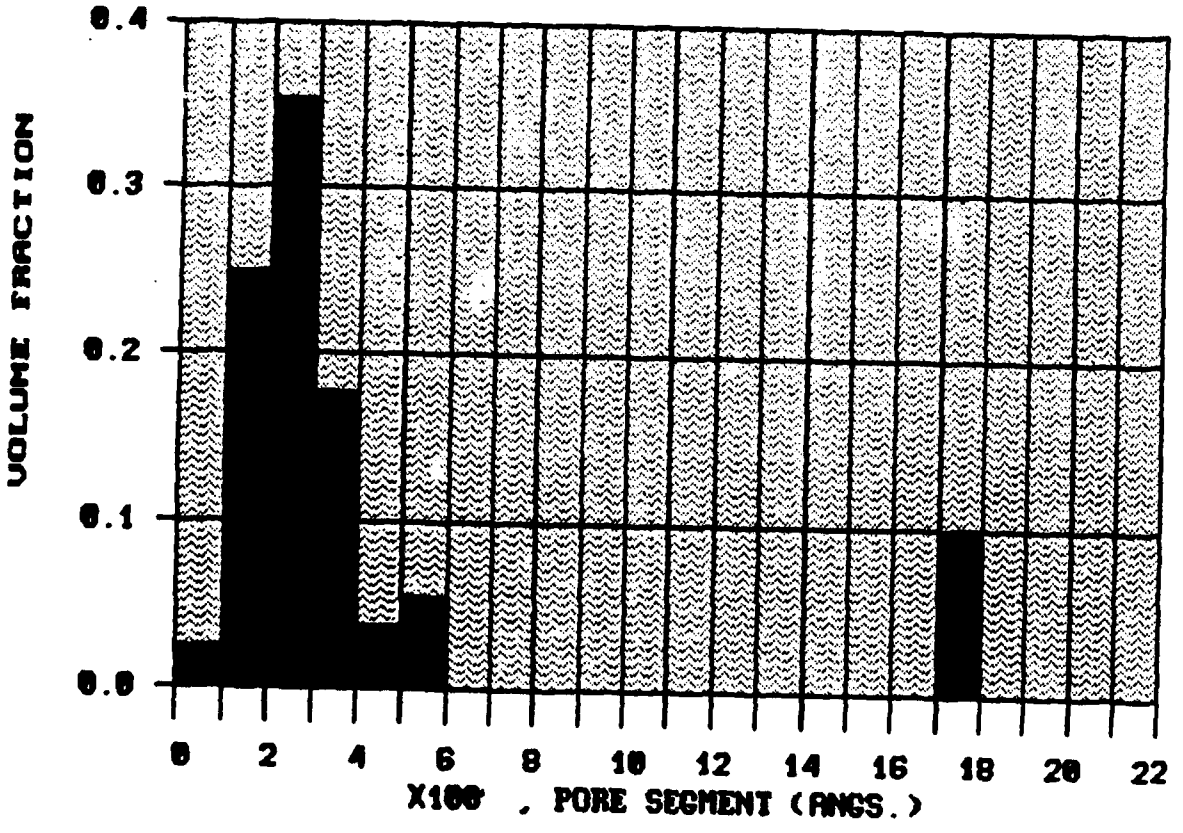

FIG.8(b) Volume distribution of pore segments

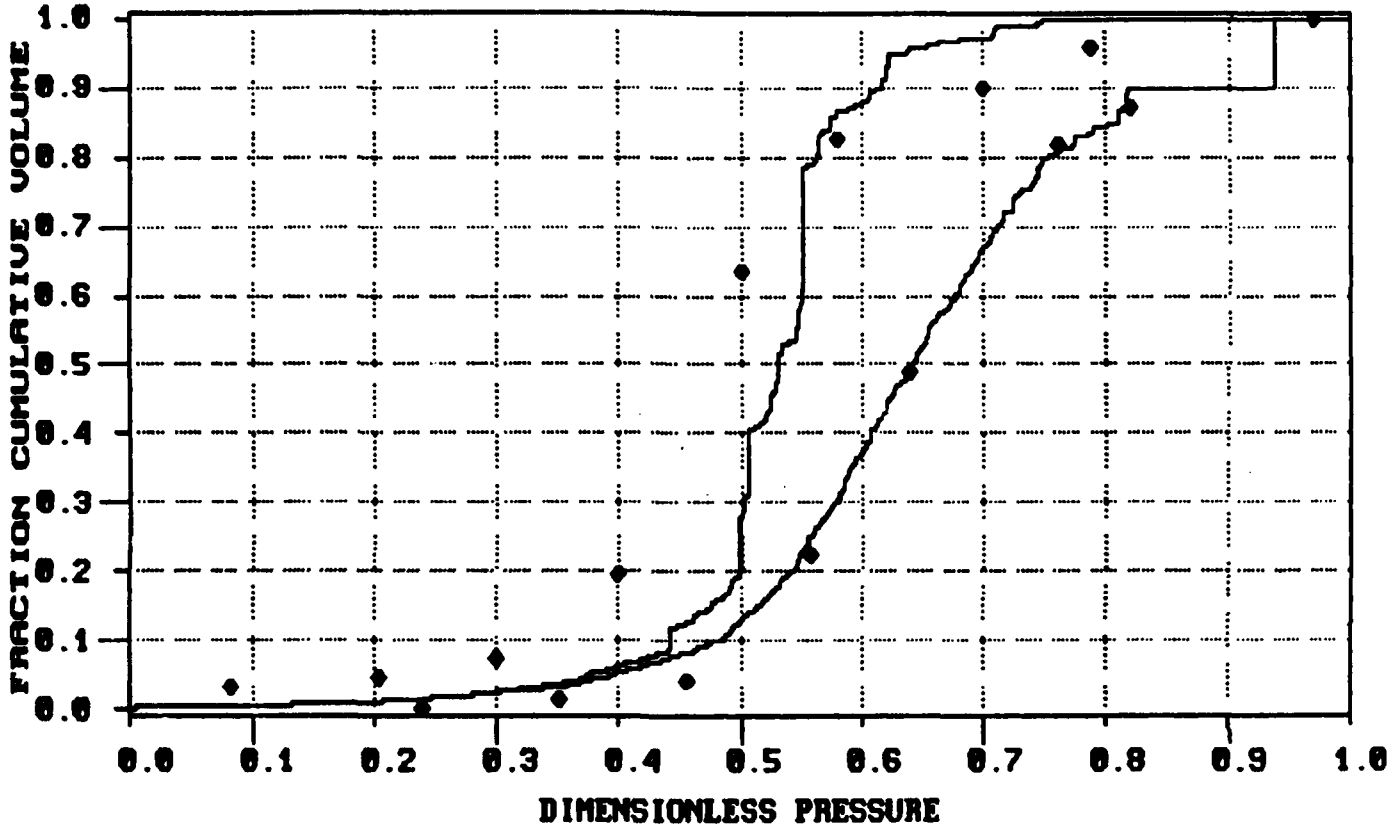

FIG.9 Predicted desorption isotherm for random network (20 x 20)

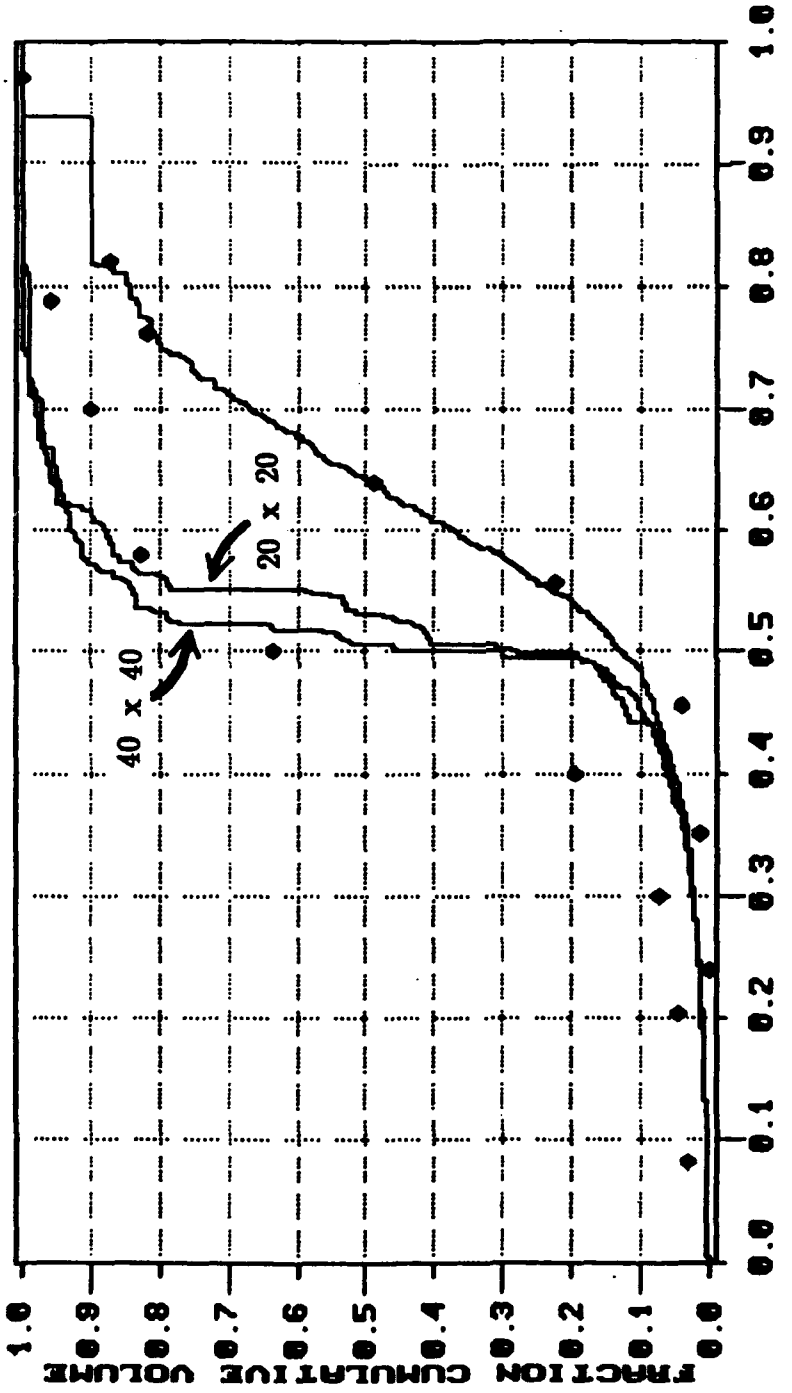

FIG.10 Comparison of desorption isotherms for random 20 x 20 and 40 x 40 networks

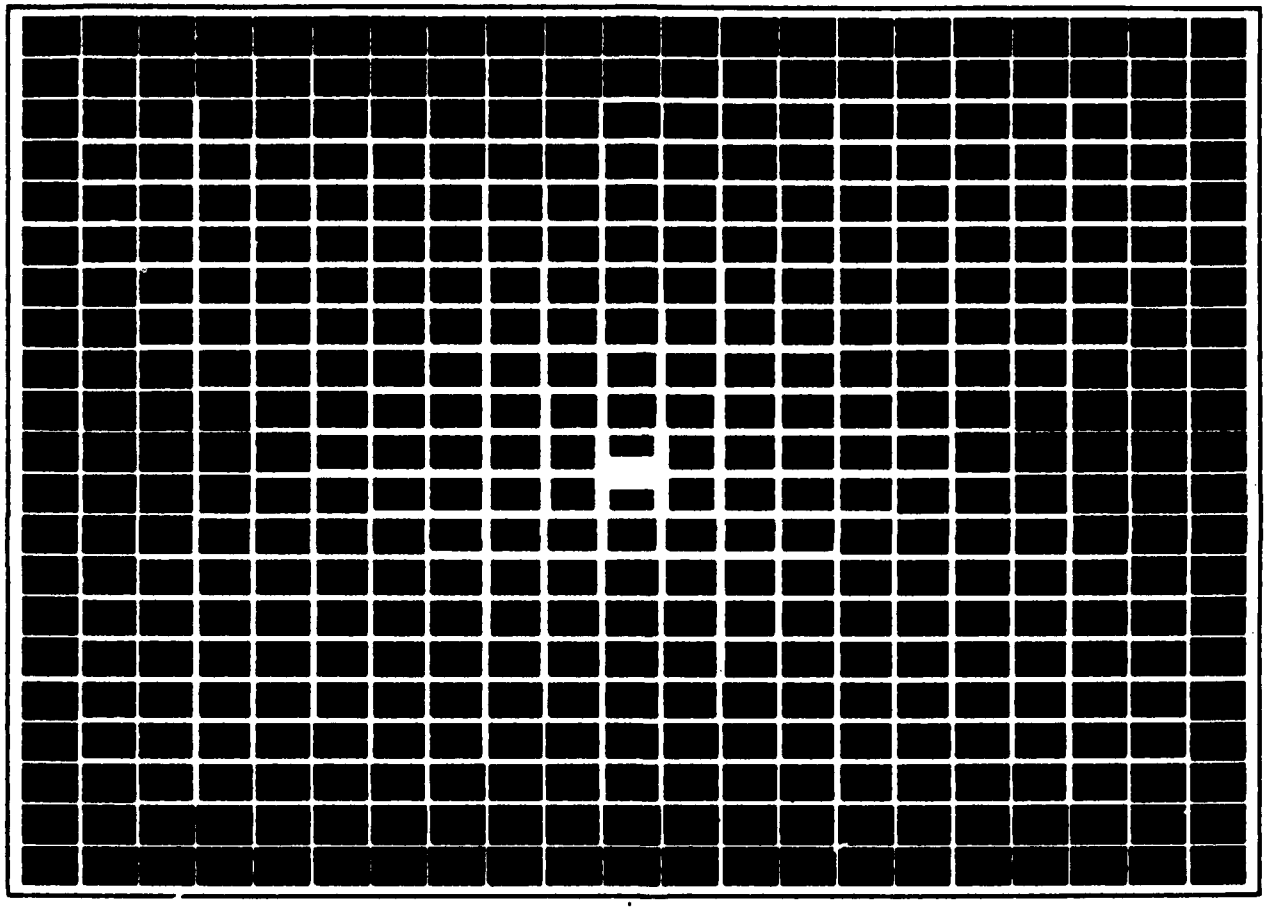

FIG.11a. Spirally wound networks of pores, largest pores on interior/smallest on exterior

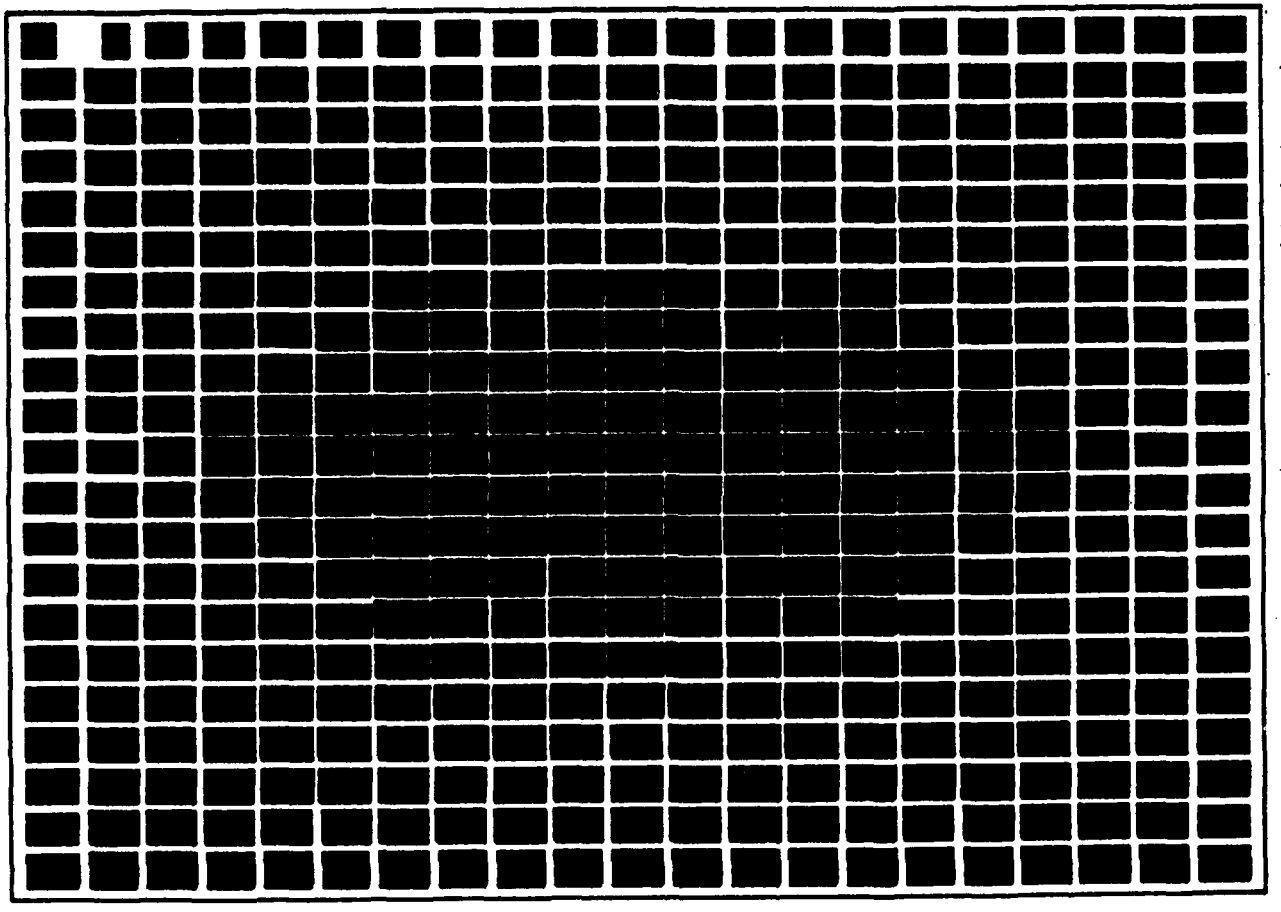

FIG.11b. Spirally wound networks of pores, smallest pores on interior/largest on exterior

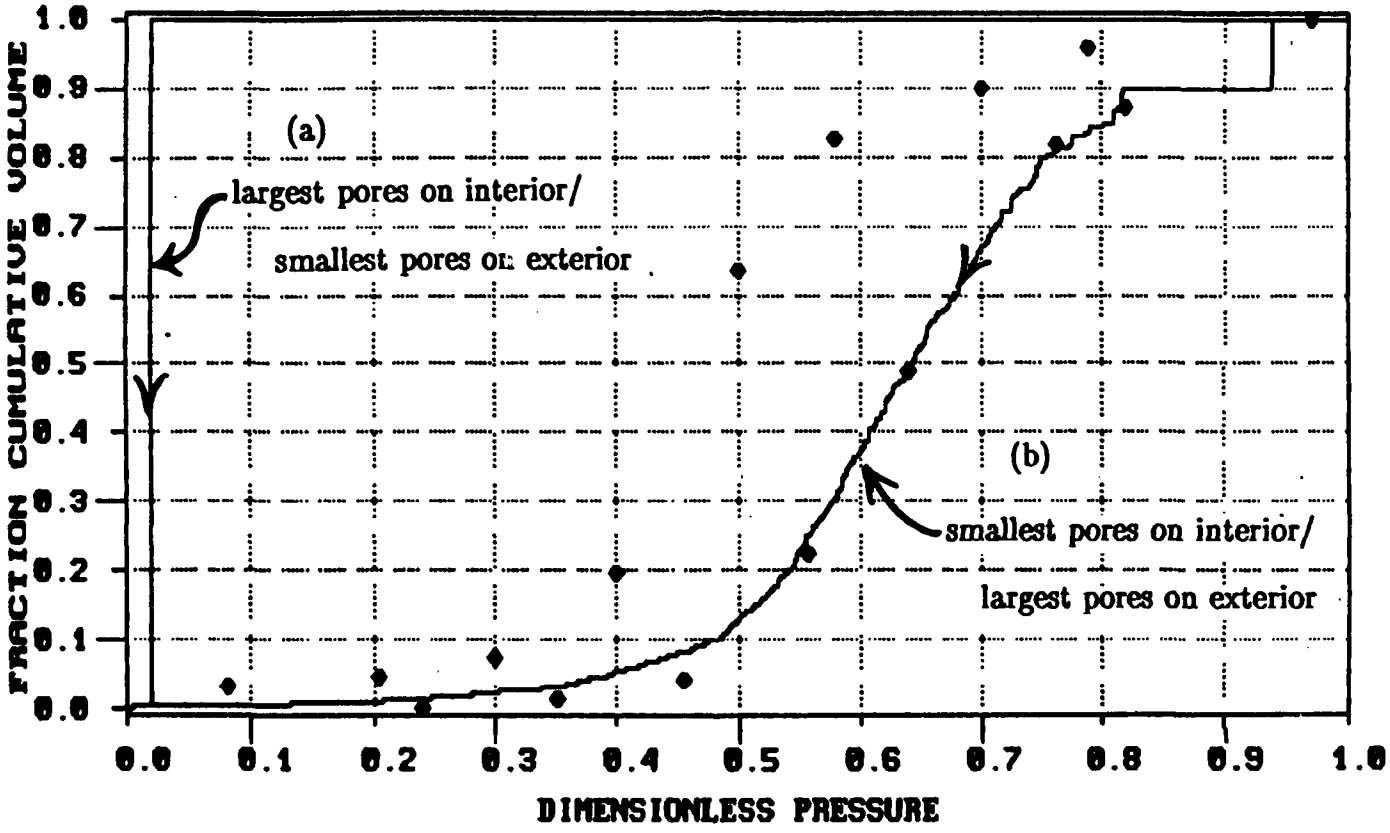

FIG.12 Predicted desorption isotherms for spiral winding of pores

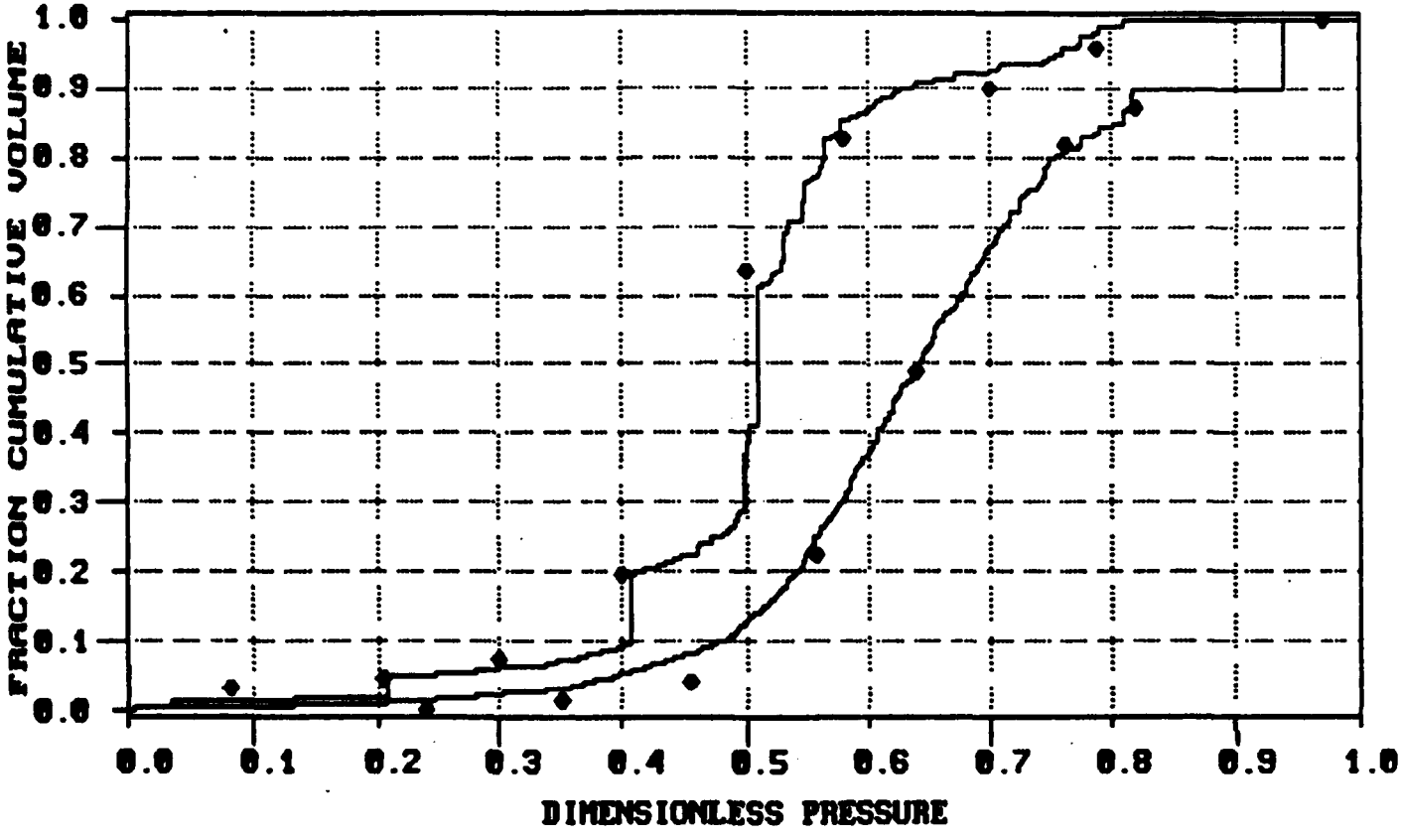

FIG.13 Isotherms predicted using patchy heterogeneity

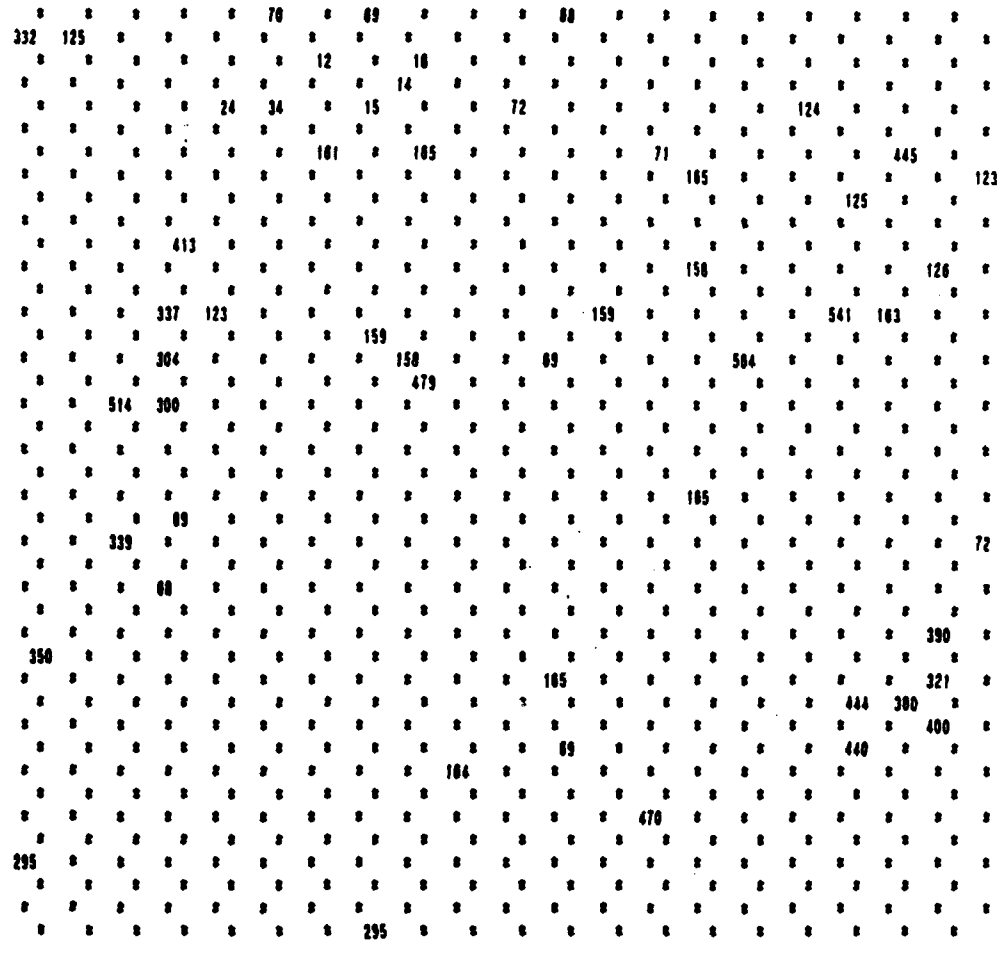

FIG.14a. Details of local reordering with patchy heterogeneity, pores subjected to repositioning

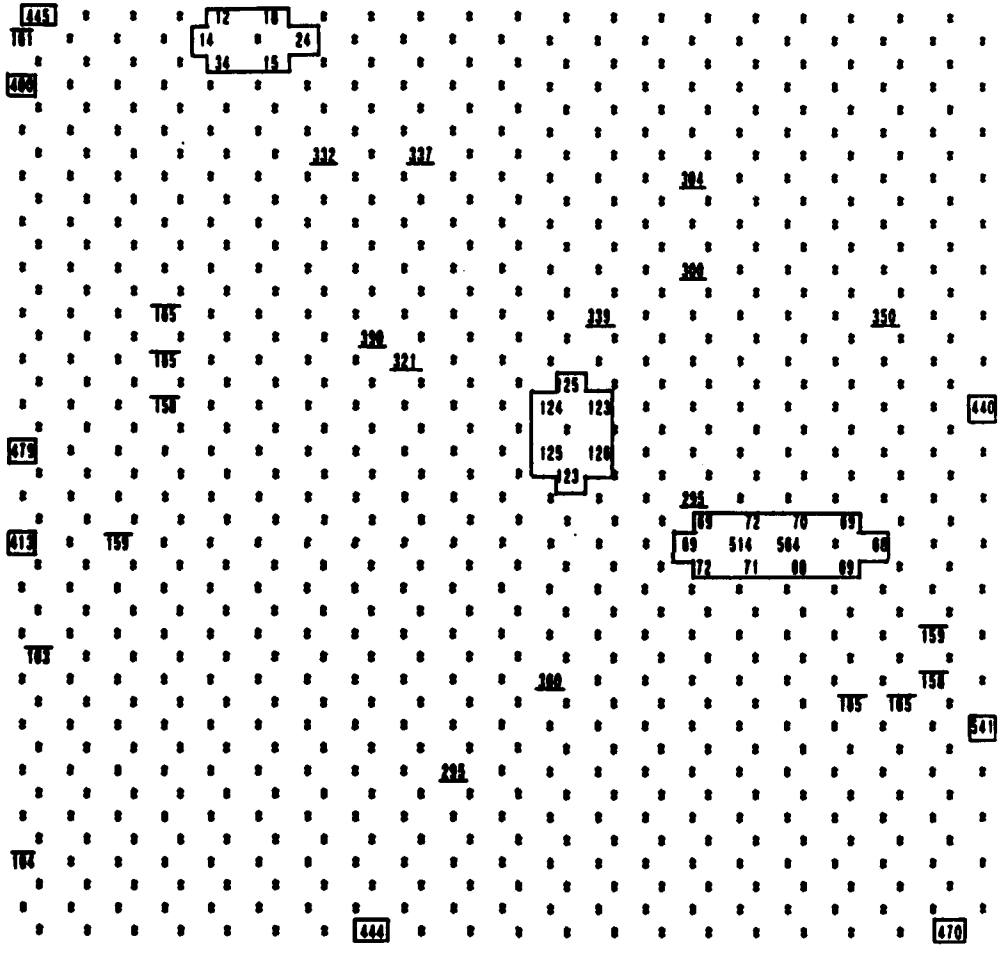

FIG. 14b. **Details of local reordering with patchy heterogeneity, pores as repositioned**

TABLE PORE EMPTYING SEQUENCE FOR SIMPLE 4 x 4 NETWORK

Emptying Range	No of Pores Emptied	Individual Pore Sizes
1000 → 900 Å	4	970, 970, 950, 900
900 → 800 Å	None	–
800 → 700 Å	3	750 → 970, 950
700 → 600 Å	None	–
600 → 500 Å	2	500, 500
500 → 400 Å	1	470
400 → 300 Å	None	–
300 → 200 Å	2	250, 250
200 → 100 Å	28	190, 190, 190 → 950, 930, 990, 880, 950, 1000, 910, 1000, 860, 830, 980, 980, 850 180, 180 170 (x5) 160 (x2) 150 (x2) 110
100 → 0 Å	None	–
Total	**40**	

LITERATURE CITED

1. Mahle, J. J. & Friday, D. K., "Water Adsorption Equilibria on Microporous Carbons Correlated Using a Modification to the Sircar Isotherm", *Carbon*, 27, pp. 835-843 (1989).

2. Everett, D. H., "Adsorption Hysteresis", in *The Solid Gas Interface* (Ed. E. Alison Flood), 1055, Marcel Dekker, New York (1967).

3. Fatt, I., "The Network Model of Porous Media I: Capillary Pressure Characteristics", *Petrol. Trans. A.I.M.E.*, 207, 144 (1956).

4. Nicholson, D., "Capillary Models for Porous Media II: Sorption-desorption Hysteresis in 3-D Networks", *Brit. J. Appl. Phys. (J. Phys. D.)* 1, 1379 (1968).

5. Mann, R. & Thomson, G., "Interpretation of Low Temperature Gas Adsorption and Desorption Using Stochastic Pore Networks", in *Adsorption: Science & Technology*, (Al. E. Rodrigues et al, Eds.) Kluwer Academic Publishers, pp. 63-77 (1989).

6. Petropoulos, J. H., Petrou, J. K. & Kanellopoulos, N. K., "Explicit Relation Between Relative Permeability and Structural Parameters in Stochastic Pore Networks", *Chem. Eng. Sci.*, 44, pp. 2967-2978 (1989).

7. Antroutsopoulos, G. P. & Mann, R., "Evaluation of Mercury Porosimeter Experiments Using a Network Pore Structure Model", *Chem. Eng. Sci.*, 34, pp. 1203-1212 (1979).

8. Mann, R. & Golshan, H., "Application of a Stochastic Network Pore Model to A Catalyst Pellet", *Chem. Eng. Comm.*, 12, pp. 377-391 (1981).

9. Mann, R., Androutsopoulos, G. P., & Golshan, H., "Application of a Stochastic Network Pore Model to Oil Bearing Rock with Observations Relevent to Oil Recovery", *Chem. Eng. Sci.* 36, pp. 337-346 (1981).

10. Sharratt, P. N. & Mann, R., "Some Observations on the Variation of Tortuosity with Thiele Modulus and Pore Size Distribution", *Chem. Eng. Sci.* 42, pp. 1565-1576 (1987).

11. Mann, R., Sharratt, P. N. & Thomson, G., "Deactivation of a Supported Zeolitic Catalyst: Diffusion, Reaction and Coke Deposition in Stochastic Pore Networks", *Chem. Eng. Sci.* 41, pp. 711-718 (1986).

12. Arbabi, S. & Sahimi, M., "Computer Simulations of Catalyst Deactivation - II. The Effect of Morphological, Transport and Kinetic Parameters on the Performance of the Catalyst", *Chem. Eng. Sci.*, 46, pp. 1749-1755 (1991).

13. Patwardhan, A. V. & Mann, R., "Effective Diffusivity and Tortuosity in Wicke-Kallenbach Experiments: Direct Interpretation Using Stochastic Pore Networks", *Trans. I. Chem. E.*, 69 Part A, pp. 205-207 (1991).

14. Mann, R. & Wasilewski, M. C., "Towards a Fractal Computer Graphic Basis for Characterisation of Catalyst Pore Structure by Image Reconstruction", *Trans. I. Chem. E.*, 68 Part A, pp. 177-184 (1990).

GLOSSARY

p	vapour phase partial pressure of sorbate
p_{psat}	saturation vapour pressure of sorbate
R	gas constant
r	pore radius
T	absolute temperature
t	adsorbed layer thickness
V_L	molar volume of adsorbed phase
σ	surface tension
θ	contact angle